Journal of Cancer Research and Clinical Oncology (2021) 147:2851–2865
https://doi.org/10.1007/s00432-021-03683-7

ORIGINAL ARTICLE – CANCER RESEARCH

Anticancer activity of *Helicobacter pylori* ribosomal protein (HPRP) with iRGD in treatment of colon cancer

Atieh Yaghoubi[1,2] · Fereshteh Asgharzadeh[3] · Aref Movaqar[1,2] · Kiarash Ghazvini[1,2] · Seyed Mahdi Hassanian[4,6] · Amir Avan[5,6] · Majid Khazaei[3,6] · Saman Soleimanpour[1,2,6]

Received: 10 April 2021 / Accepted: 5 June 2021 / Published online: 12 June 2021

Abstract

Purpose As the conventional therapeutic approaches were not completely successful in the treatment of colon cancer, there is still a need for finding the most efficient therapeutic agents. Here we investigated the anticancer activity of HPRP-A1 that was derived from the N-terminal region of Helicobacter pylori ribosomal protein L1 (RpL1) alone or in combination with tumor-homing peptide iRGD and 5-Fluorouracil (5FU) on colon cancer cell lines (CT26 and HT29) and isograft models of colon cancer.

Method We assessed the tumor growth inhibitory activity of HPRP-A1 with or without iRGD and 5FU on colon cancer in vitro and in vivo. In the in vitro part, we investigate the effect of HPRP-A1 alone and in combination with iRGD/5FU.

Results Our results demonstrated that co-administration of HPRP-A1 with iRGD increased the apoptosis, while these two peptides in combination with 5FU increased the intracellular level of p53 that upregulate the pro-apoptotic gene BAX and downregulate the anti-apoptotic gene BCL2. HPRP-A1 blocks the cell cycle progression in G0/G1. Co-administration of two peptides significantly reduced the size and weight of the tumors, while the group that received 5FU in combination with the peptides increased the necrotic and decrease the fibrotic area significantly in the tumor tissues, which also disrupt the oxidant/antioxidant balance.

Conclusions Our results indicated that HPRP-A1 could be considered an effective agent toward colon cancer in vitro and in vivo with the ability to enhance the effects of conventional chemotherapy agent 5FU.

Keywords HPRP-A1 · Bacterial peptide · Colon cancer · iRGD

Introduction

Colon cancer is one of the most commonly diagnosed cancers among men and women, with over one million new cases in 2020 (Siegel et al. 2020). Surgery, chemotherapy, and antibody therapies have long been the first choices for colon cancer (Cao et al. 2009). However, these conventional therapeutic approaches cannot be completely successful in the treatment of colon cancer due to some disadvantages, such as non-specific toxicity to normal cells and the formation of multi-drug resistant (MDR) cells in the case of using some chemotherapeutic agents (Cao et al. 2009). Lesions

Atieh Yaghoubi and Fereshteh Asgharzadeh contributed equally to this work.

✉ Majid Khazaei
Khazaeim@mums.ac.ir

✉ Saman Soleimanpour
soleimanpours@mums.ac.ir

[1] Antimicrobial Resistance Research Center, Bu-Ali Research Institute, Mashhad University of Medical Sciences, Mashhad, Iran

[2] Department of Microbiology and Virology, Faculty of Medicine, Mashhad University of Medical Sciences, Mashhad, Iran

[3] Department of Physiology, Faculty of Medicine, Mashhad University of Medical Sciences, Mashhad, Iran

[4] Department of Medical Biochemistry, Faculty of Medicine, Mashhad University of Medical Sciences, Mashhad, Iran

[5] Department of Medical Genetics and Molecular Medicine, Faculty of Medicine, Mashhad University of Medical Sciences, Mashhad, Iran

[6] Metabolic Syndrome Research Center, Mashhad University of Medical Sciences, Mashhad, Iran

that commonly occur in advanced colon cancer extend to the peritoneal cavity and lead to multiple metastatic lesions. Chemotherapeutic agents and antibody therapy agents cannot penetrate into these lesions since they lead to decreasing the patient's survival rate (Lemoine et al. 2016; Sugarbaker 2016). Hence, there is an urgent need for novel therapeutic agents to combat this cancer. Currently, utilizing bacteria has attracted much attention as a new approach for cancer therapy. Bacillus Calmette–Guérin (BCG) was another example of using bacteria for the treatment of cancer in the 1970s. BCG is the attenuated form of *Mycobacterium bovis* strain that received FDA approval for intravesical therapy of patients with non-muscle-invasive bladder cancer (NMIBC) (Gontero et al. 2010). In current investigations, different forms of bacteria such as live, attenuated, or genetically modified states, and their products (including bacterial peptides, bacteriocins, and toxins) are used in the treatment of several types of cancer (Boohaker et al. 2012; Roberts et al. 2014; Fujimori 2006). Some species of bacteria with anticancer potential are *Lactococcus*, *Clostridia*, *Shigella*, *Bifidobacteria*, *Listeria*, *Vibrio*, *Salmonella*, and *Escherichia* (Lax 2005; Lecuit et al. 2004; Gupta et al. 2016; Nath et al. 2010). Current studies suggest that these species are able to invasion the tumors then colonization into them, which led to tumor suppression and inhibits the proliferation of neoplasm (Wei et al. 2007; Chang et al. 2015; Hetz et al. 2002; Yan et al. 2015). The hypoxic and necrotic area of the tumor causes the resistance of the tumor to the conventional therapy agents, thus influences the outcome of treatment. However, some bacteria including *Clostridia* strains and *Bifidobacterium longum* can inter to this area, survive under hypoxic conditions then colonize and caused tumor destruction (Roberts et al. 2014; Fujimori 2006). Currently, some studies by genetic engineering try to produce more effective bacterial-based therapy agents with minimal adverse effects. Attenuated form of auxotrophic mutants of the *Salmonella typhimurium* (*S. typhimurium*) is one of these examples which selectively invade the tumor cells and inhibit the tumor growth, also it is able to proliferate within the necrotic and hypoxic area of the tumor (Zhao et al. 2006). Recent findings of using bacterial peptides in the treatment of cancers have attracted considerable attention due to their therapeutic advantages. These peptides can prevent the formation of multidrug-resistance cells and improve the anticancer effect of conventional therapeutic agents (Boohaker et al. 2012; Marqus et al. 2017). The recent finding suggests that bacterial peptides are very potent in inhibiting the proliferation of cancer cells. Furthermore, bacterial peptides have specific toxicity and penetrating ability for tumor cells with low accumulation in tissues. The small size, easily modifiable features, and rapid, generally simple synthesis are other advantages of bacterial peptides (Marqus et al. 2017).

According to various reports, small peptides derived from the N-terminal region of *Helicobacter pylori* (*H. pylori*) ribosomal protein L1 (RpL1) have anticancer potential (Pütsep et al. 1999; Kang et al. 2005). L1 protein can directly bind to 23SrRNA. The stalk of L1 protein is very mobile in the ribosome and is involved in the E site tRNA release. L1 protein has a role as a translational repressor protein, and also it controls the translation of the L11 operon by binding to its mRNA. This derived peptide called HPRP-A1 (FKKLKKLFSKLWNWK) shows anticancer activity through different mechanisms (i) activation of caspase-3, -8 and -9-dependent pathway leading to apoptosis, (ii) arresting the cell cycle at the G0/G1 and G2/M, (iii) cell proliferation inhibition, (iv) damaging the mitochondrial function, and (v) increasing the generation of reactive oxygen species (ROS) (Hu et al. 2018a, b, c; Hao et al. 2019). One of the key challenges in the fields of peptide-based therapy of cancer is the short half-life of these agents. Currently, tumor-penetrating peptides (TPPs) are discovered, allowing the selective delivery of therapeutic agents to the tumors that are also used to enhance the bacterial peptide half-life (Teesalu et al. 2013; Ruoslahti 2017). A cyclic peptide with a length of 9 amino acids, called iRGD (CRGDKGPDC), is widely used as a TPPs (Sugahara et al. 2010). This cyclic peptide can enter into the tumors by binding to αVβ3 and αVβ5 integrins and then cleaved by the protease, leading to the activation of revealing the c-terminal CendR motif (R/KXXR/K) of the peptide. This motif activates the endocytotic/exocytotic transport pathway through binding to the neuropilin-1 (NRP-1) that enhances the transport of co-administered anti-cancer drugs into tumors (Teesalu et al. 2009). In the present study, we aimed to investigate the anticancer effect of HPRP-A1 with or without the tumor-targeting peptide iRGD and 5 Fluorouracil (5FU) as a standard drug on colon cancer in vitro and in vivo.

Materials and methods

Peptide synthesis and purification

The anticancer peptide HPRP-A1 (Ac-FKKLKKLFSKLWNWK-amide) and homing peptide iRGD (Ac-CRGDKGPDC-amide) were synthesized by ProteoGenix Inc. at > 95% purity and mass balance. In addition, iRGD is a disulfide-based cyclic peptide. The reaction was oxidized by thallium trifluoroacetate on solid-phase resin after the linear chain amino acid was completed. The purified peptides were further characterized by mass spectrometry and amino acid analysis.

Cell culture

In this study, we used two colon cancer cell lines, including CT26 (murine colorectal carcinoma cell line) and HT29 (human colon cancer cell line). One of the cell lines that was used in this study was CT26 that is a murine colorectal carcinoma cell line that is from a BALB/c mouse. This cell line suitable for in vitro and in vivo experimentation. CT26 cells will form tumors and metastases post-implantation into syngenic BALB/c mice or immunocompromised mice (Abedizadeh et al. 2020; Zhang et al. 2013). Another cancer cell line we used was HT29 which is a human colorectal adenocarcinoma cell line with epithelial morphology. This cell line sensitive to the chemotherapeutic drugs 5-fluorouracil and oxaliplatin, which are standard treatment options for colorectal cancer. Furthermore, HT29 is used widely as an in vitro model to study absorption, transport, and secretion by intestinal cells, in addition, this cell line is used in the in vivo studies to induce the xenograft tumor model of colorectal cancer (Cohen et al. 1999). Under standard culture conditions, HT29 grows as a nonpolarized, undifferentiated multilayer, while changing the culture conditions or treating cells with various inducers caused differentiated and polarized morphology that characterized by the redistribution of membrane antigens and development of an apical brush-border membrane (Nautiyal et al. 2011). We also used a normal fibroblast cell line L929. All the cell lines were cultured in Roswell Park Memorial Institute (RPMI) 1640 (Gibco Life Technologies, Thermo Fisher Scientific, MA, USA) with fetal bovine serum (FBS) (10% v/v), penicillin (100 U/ml), and streptomycin (100 U/ml) in a humid atmosphere at 37 °C with 5% CO2.

Cell viability assay

In this respect, we cultured the CT26, HT29, and L929 cell lines in a 96-well culture plate for 24 h. After the incubation time, all the three cell lines were exposed to six different groups of treatments, including (i) HPRP, (ii) HPRP + iRGD, (iii) HPRP + 5FU, (iv) HPRP + 5FU + iRGD, (v) iRGD, and (vi) 5-Fluorouracil (5FU) (Ebewe Pharma, Austria) at various concentrations incubated at 37 °C with 5% CO2 for 24 h. Then, MTT was added (0.05 mg/ml, 100 µl per well), and the cells were incubated for another 4 h at 37 °C. In the next step, the supernatant was removed, and DMSO was added (100 µl per well) to dissolve the formazan crystals. Ultimately, the absorption at 540 nm was measured by a microplate reader (TECAN NanoQuant Infinite M200 Microplate Reader, USA). The MTT assays were performed in triplicates (Amerizadeh et al. 2018).

Flow cytometric analysis of apoptosis

An annexin V-FITC/PI double staining method was used for the apoptosis assay. In brief, CT26 and HT29 cells were exposed to the HPRP-A1 with or without iRGD and 5FU for 24 h. At the end of the treatment, the cells were trypsinized, washed with PBS, and centrifuged at 400 × g for 5 min. Then, the cells were resuspended in 90 µL of binding buffer and stained with 5 µL annexin V-FITC and 5 µL PI (Incubate 20 min in the dark). Finally, the stained cells were collected for flow cytometric analysis using the FACSCalibur flow cytometer (Giovannetti et al. 2014).

Cell cycle analysis by flow cytometry

In this regard, CT26 and HT29 cells were seeded ($2–3 \times 10^5$ cells/well) in the 6-well plates at 37 °C, 5% CO2. After 24 h, the cells were exposed to six different treatment groups, including HPRP, HPRP + iRGD, HPRP + 5FU, HPRP + 5FU + iRGD, iRGD, and 5FU. After the incubation time, 100 µg/ml stock of RNase A was added and incubated at 37 °C for 30 min. Then, the cells were mixed with propidium iodide (PI, 50 µg/ml) and incubated at 24 °C for 20 min. In the end, the stained cells were collected for the flow cytometric analysis using the FACSCalibur flow cytometer, and the cell cycle was then analyzed using FlowJo V10_CL software (Marjaneh et al. 2018).

Migration assay

For the migration assay, we used the wound healing assay (scratch assay). In brief, CT26 and HT29 cells were cultured at 37 °C, 5% CO2, and grown to achieve 70% confluence. Then, the cells were scratched with a p200 pipette tip, and the free detached cells were then removed with PBS. The scratch area was measured using a 10 × objective (ZEISS Microscopy, Germany). The non-transfected cells were used as a control group to assess the migration of transfected cells. The wound healing rate was measured via the ImageJ software (NIH, Bethesda, MD). All the assays were performed in triplicates, and significant changes among transfected and non-transfected cells were assessed by the ANOVA test.

Antitumor efficacy in isograft mice

Seven-week-old female inbred Balb/C mice were bought from Pasteur Institute (Tehran, Iran) and were housed in standard conditions approved by Animal Ethics Committee Institute (temperature 22 ± 2 °C, the humidity of 54 ± 2%, and 12 h light/dark cycle). All the protocols were according to the guidelines of Care and Use of Animals Laboratory, approved by the Ethics Committee of Mashhad University

of Medical Sciences. CT26 cells (2×10^6) were subcutaneously injected into the left flank of the mice. The isograft mice were randomly divided into seven groups ($n=6$ for each group) when the tumors grew to 80–100 mm^3. The groups included (i) Control group (tumor without treatment); (ii) 5FU (treated with 5 mg/kg every other day, intraperitoneal "ip" injection); (iii) HPRP (10 mg/kg/every 2 days "direct injection into the tumor"); (iv) iRGD (5 mg/kg/every 2 days "direct injection"); (v) HPRP + iRGD (10 and 5 mg/kg/ every 2 days, respectively "direct injection"); (vi) HPRP + 5FU (10 mg/kg/every 2 days "direct injection" and 5 mg/kg every other day "ip", respectively); (vii) HPRP + iRGD + 5FU (10 and 5 mg/kg/every 2 days "direct injection" and 5 mg/kg/every other day "ip", respectively") (Hao et al. 2019; Hu et al. 2018d; Hamilton et al. 2015; Marjaneh et al. 2018). The tumor size was measured every other day using a digital caliper and by the following formula: Tumor volume $= \left(\text{tumor length} \times \text{tumor width}^2\right)/2$. At the end of the experiment, mice were dissected. Tumor tissues and major organs (heart, liver, lungs, and kidneys) were dissected out, fixed in 10% formalin, embedded in paraffin, and sectioned at a thickness of 5 µm. The sections were stained with Hematoxylin–Eosin (H&E) and Masson's trichrome stains and studied under light microscopy (×40 magnification). The percentage of necrosis and fibrosis was measured by ImageJ software (NIH, Bethesda, MD).

Oxidative/antioxidative stress markers assessment

For this purpose, the homogenized tumor tissues were used for the assessment of oxidative markers, including malondialdehyde (MDA), as well as antioxidative markers such as total thiol groups (SH), catalase (CAT) activity, and superoxide dismutase (SOD).

Malondialdehyde (MDA)

Malondialdehyde (MDA) is considered a biomarker of lipid peroxidation. For determining the MDA level, 1 ml of 10% (weigh tissue/ volume of saline) tumor tissue homogenates were mixed with 2 mL of thiobarbituric acid (TBA), trichloroacetic acid (TCA), and HCL solution in boiling water. In the next step, the absorbance was measured at 535 nm wavelength by using a spectrophotometer (Amerizadeh et al. 2018).

Total thiol group

The SH level was assessed by DTNB (Di-Tio nitro benzoic acid) reagent, which reacted with SH groups and led to the production of the yellow color complex. In this manner, tumor tissue supernatant was incubated with DTNB in Tris–EDTA buffer (pH = 8.6). Then, this mix was for 10 min at room temperature. In the next step, absorbance was measured at 412 nm wavelength. The total thiol content was calculated using this formula. $(\text{Total thiol concentration (mM)} = (A2 - A1 - B) \times 1.07/(0.05 \times 13.6))$ (Marjaneh et al. 2018).

Superoxide dismutase

In this manner, pyrogallol autoxidation is characterized by inhibition of the conversion of MTT to formazan that was based on the measurement of SOD activity. The formazan was dissolved in DMSO and the absorbance was read at 570 nm wavelength (Elmi et al. 2008).

Catalase

Catalase activity was measured by Aebi et al. based on the hydrolyzation of H_2O_2 in phosphate buffer, pH = 7.0, and reducing absorbance at 240 nm. The activity of CAT obtained through the conversion of H_2O_2 to H_2O and O_2 in 1 min under a standard situation (Aebi 1984; Marjaneh et al. 2018).

RNA isolation and real-time PCR

We used FavorPrep™ Tissue Total RNA Mini Kit for extracted total RNA from tumor tissue purchased from Favorgen Biotech (Taiwan). The cDNA Synthesis Kit obtained from Yekta Tajhiz (Tehran, Iran) was used for cDNA synthesis. The Ampliqon SYBR Green PCR Master Mix was applied for quantitative real-time PCR reactions. The expression levels of the genes were normalized

Table 1 qPCR primer sequences

Gene	Source	Primer	Sequence
GAPDH	Mouse	Forward	CAACGACCCCTTCATTGACC
		Reverse	CTTCCCATTCTCGGCCTTGA
P53	Mouse	Forward	GGACAGCTTTGAGGTTCGTG
		Reverse	TCATTCAGCTCCCGGAACAT
BAX	Mouse	Forward	AGACAGGGGCCTTTTTGCTAC
		Reverse	AATTCGCCGGAGACACTCG
BCL2	Mouse	Forward	GCTACCGTCGTCGTGACTTCGC
		Reverse	CCCCACCGAACTCAAAGAAGG
Col1a2	Mouse	Forward	GTTCTCAGGGTAGCCAAGGT
		Reverse	CCTTCAAAACCAAAGTCATAGCC
Col1a1	Mouse	Forward	TGACGCATGGCCAAGAAGA
		Reverse	CAGATCAAGCATACCTCGGG
MCP-1	Mouse	Forward	GTGAAGTTGACCCGTAAATCTGA
		Reverse	ACTAGTTCACTGTCACACTGGT
IL1β	Mouse	Forward	GACTTCACCATGGAATCCGT
		Reverse	TGCTCATTCACGAAAAGGGA

to a housekeeping control gene (GAPDH) (Dinarvand et al. 2015). The primer sequences are shown in Table 1.

Statistical analysis

The average data were presented as the means ± standard error and the Student's t-test or ANOVA followed by Tukey's multiple comparison tests were used for the data analysis via SPSS Ver.0.20 statistical software (IBM, Chicago). Statistical significance was lower than 0.05.

Results

In vitro anticancer activity and cytotoxicity

We used MTT assay to determine the effect of HPRP with or without iRGD and 5FU on the cell viability of CT26, HT29, and L929 cell lines. The results were calculated with CalcuSyn software (Ver.2.0). Hence, cells were exposed to the various concentrations of HPRP with or without 6 µg/ml iRGD and 3.84×10^{-5} M 5FU for 24 h. The cell viability of CT26 and HT29 cell lines were significantly decreased along with the increasing concentration of HPRP peptide. The cell viability of CT26 and HT29 were decreased after exposure to the high concentration of iRGD, while we observed the stronger cytotoxic activity at the time of using in combination with HPRP. The cell viability of the HT29 cell line decreased significantly, along with the increasing concentration of peptides. In contrast, it declined slowly on the CT26 cell line, suggesting that the HT29 cell line was more sensitive to the peptide combination. In addition, exposure to 0.73 µg/ml HPRP-A1 with or without 6 µg/ml of iRGD and 3.84×10^{-5} M 5FU for 24 h did not decrease the proliferation (< 5%) of normal fibroblast cells (Fig. 1).

Flow cytometric analysis of apoptosis

The early and late apoptosis of HPRP-A1 with or without iRGD and 5FU was determined by using the FITC Annexin V/PI apoptosis detection kit. The flow cytometry results were analyzed by using FlowJo (Ver. 10) software. iRGD is a tumor-homing and penetrating peptide that is also known as an apoptosis-inducing peptide (Qifan et al. 2016; Sugahara et al. 2009). Our results demonstrate that the apoptotic activity of HPRP significantly increases after co-administration by iRGD with or without 5FU in both cancer cell lines in comparison to the control group and when the cells received the single therapy ($P < 0.001$) (Fig. 2). Furthermore, HPRP-A1 with or without iRGD and/or 5FU significantly increased the expression of BAX in the tumor tissue as compared to the

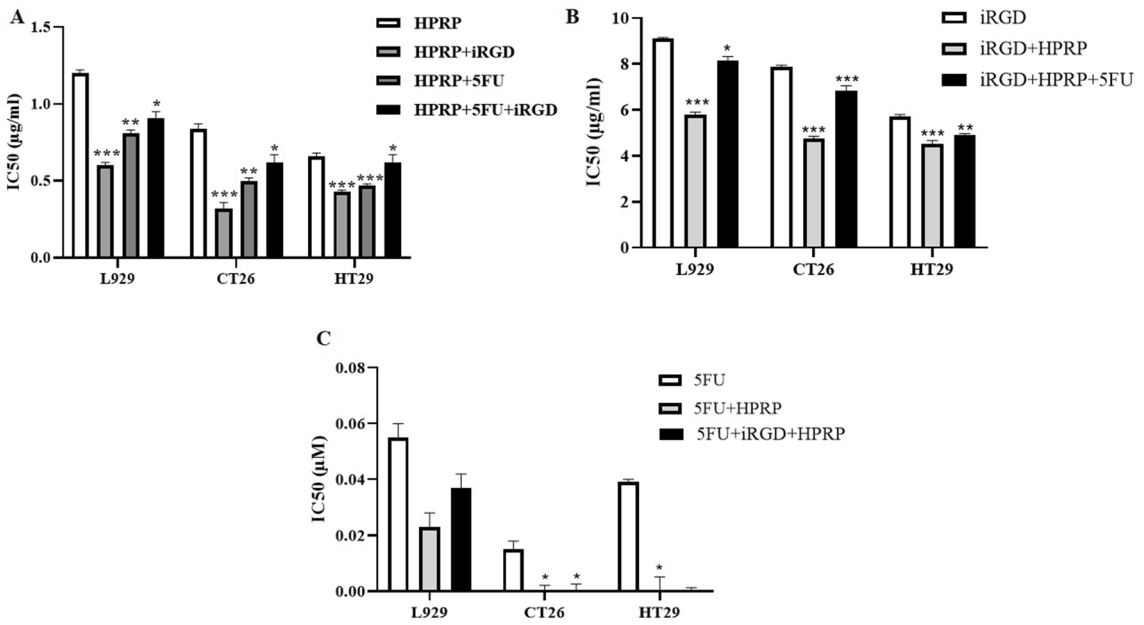

Fig. 1 IC50 values in L929, CT26, and HT29 cells treated with peptides. **A** IC50 values of HPRP-A1 with or without iRGD and 5FU at the indicated concentration were measured by MTT assay after 24 h. **B** IC50 values of peptide iRGD with or without HPRP-A1 and 5FU at the indicated concentration were measured by MTT assay after 24 h. **C** IC50 values of peptide 5FU with or without iRGD and HPRP-A1 at the indicated concentration were measured by MTT assay after 24 h. (*$P < 0.05$; **$P < 0.01$; and ***$P < 0.001$; in compare to when cell lines treated with peptides or 5FU alone)

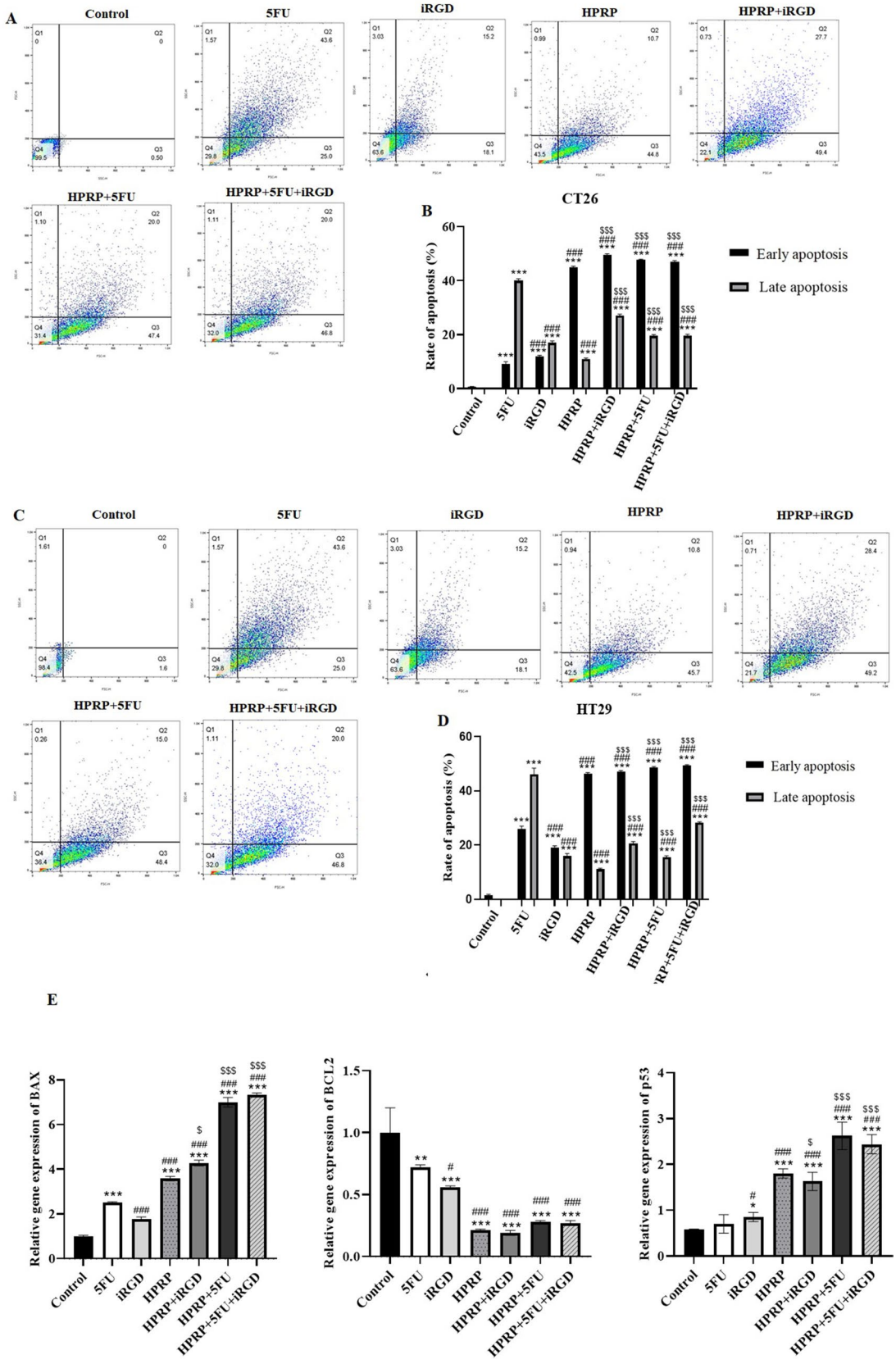
A
Control
5FU
iRGD
HPRP
HPRP+iRGD
HPRP+5FU
HPRP+5FU+iRGD
B
CT26
Rate of apoptosis (%)
Early apoptosis
Late apoptosis
C
HT29
D
E
Relative gene expression of BAX
Relative gene expression of BCL2
Relative gene expression of p53

◂**Fig. 2** Apoptosis induction activity of peptides in CT26 and HT29 cells. **A** CT26 cell lines were exposed to the 0.73 µg/ml HPRP-A1 with or without 6 µg/ml iRGD and 3.84×10^{-5} M 5FU for 24 h. The early and late apoptotic rates were measured by flow cytometry. **B** The percentage of cells in early and late apoptosis in CT26 cells incubated with peptides as indicated in (**A**). **C** HT29 cell lines were exposed to the HPRP-A1 with or without iRGD and 5FU for 24 h. The early and late apoptotic rates were measured by flow cytometry. **D** The percentage of cells in early and late apoptosis in HT29 cells incubated with peptides as indicated in (**A**). **E** The expression level of BAX, BCL2, and p53 in the tumor tissue. (*$P<0.05$, **$P<0.01$ and ***$P<0.001$ compare to control group); (#$P<0.05$ and ###$P<0.001$ compare to 5FU group); and ($$P<0.05$ and $$$$P<0.001$ compare to HPRP-A1 group)

control group ($P<0.001$). However, combination therapy of HPRP-A1with iRGD and 5FU significantly increased the expression of BAX compare to when experiments received the peptides alone ($P<0.001$). In addition, HPRP-A1with or without iRGD and/or 5FU significantly reduced the expression level of BCL2 in comparison to the control and 5FU group in the tumor tissue ($P<0.001$) (Fig. 2E).

HPRP-A1 blocks cell cycle progression in G0/G1

The cell cycle analysis indicated that co-administration of HPRP-A1 with iRGD and 5FU induced a G1 arrest in both the CT26 and HT29 cells (88.8% and 87.7%, respectively). Furthermore, co-administration of 0.73 µg/ml HPRP-A1 with 6 µg/ml of iRGD and 3.84 × 10-5 M 5FU results in much higher numbers of cells in sub-G1 of the CT26 and HT29 cells (32.8% and 45.1%, respectively) compared to when the cells are only exposed to the HPRP-A1 (20.6% and 25%, respectively) (Fig. 3). In addition, HPRP-A1 with or without iRGD and 5FU significantly increased the p53 in the tumor tissues in comparison to the control and 5FU groups ($P<0.001$). Furthermore, co-administration of HPRP-A1 by 5FU with or without iRGD significantly elevated the level of the p53 in the tumor tissues in comparison to the group that was treated with HPRP-A1 alone ($P<0.001$) (Fig. 2E).

Migration assay

Our results demonstrated that the migration and invasion rates of the cells are significantly decreased after being treated with 0.73 µg/ml HPRP-A1 and 6 µg/ml of iRGD after 24 h (Prevention rate: CT26, 25.68% and HT29, 19%) ($P<0.001$) (Fig. 4). Furthermore, combination therapy of HPRP-A1 along with 5FU also significantly reduces the migration rate of cells in comparison to when cells treated with HPRP-A1 or 5FU alone (Prevention rate: CT26, 30.65% and HT29, 22.53%) ($P<0.05$) (Fig. 3).

In vivo tumor-suppressive activity

Our results demonstrated that combination therapy of HPRP-A1 with or without iRGD significantly reduced the tumor size and weight in comparison to the control group ($P<0.001$). Furthermore, co-administration of HPRP-A1 and iRGD with or without 5FU also significantly decreased the tumor size and weight in comparison to the control group ($P<0.01$) (Fig. 5). The result of the H&E staining of tumor tissues indicated that combination therapy of HPRP-A1 and 5FU with or without iRGD significantly increased the necrotic area in the tumor tissue in comparison to the control group and when the experiments received 5FU and HPRP-A1 alone ($P<0.001$ and $P<0.01$, respectively) (Fig. 6). In addition, trichrome staining result showed that combination therapy of HPRP-A1 and 5FU with or without iRGD significantly reduced the fibrotic area and collagen accumulation in the tumor tissue in comparison to the control group and the group that received 5FU or peptide alone ($P<0.001$) (Fig. 7A and B). Moreover, the expression of CoL1a2 genes was significantly reduced in the experiments treated with HPRP-A1 and iRGD as compared to the control group and when isograft treated with 5FU or peptide alone ($P<0.001$) (Fig. 7D). However, the expression of CoL1a1 was significantly decreased in the HPRP-A1 + iRGD group as well as the HPRP-A1 + 5FU group in comparison to the control group and group that received only HPRP-A1 or 5FU ($P<0.001$) (Fig. 7C). The H&E result of the primary organs (heart, liver, lung, and kidneys) of each group determined that there were no obvious changes in these organs after treatment with single or combination peptides (Fig. 6C).

The effects of HPRP-A1 on oxidant/antioxidant balance and inflammation

Assessment of the oxidant/antioxidant balance in the tumor tissue homogenates demonstrated that HPRP-A1with or without in the tumor tissues as compared to the control group ($P<0.001$) (Fig. 8A). However, the combination therapy of HPRP-A1 with iRGD and 5FU significantly reduced the level of anti-oxidant markers including thiol, catalase, and SOD activity in comparison to the control group and when the experimental group was treated with 5FU or peptides alone ($P<0.001$) (Fig. 8). Moreover, the expression level of a pro-inflammatory gene such as IL1β was significantly increased in the experimental group that received HPRP-A1 along with iRGD and 5FU in comparison to the control group and when the experimental group was treated with peptides or 5FU alone ($P<0.001$and $P<0.01$, respectively) (Fig. 8E). HPRP-A1 with or without iRGD and 5FU significantly reduced the expression level of the pro-fibrotic gene MCP-1 as compared to the control group ($P<0.001$).

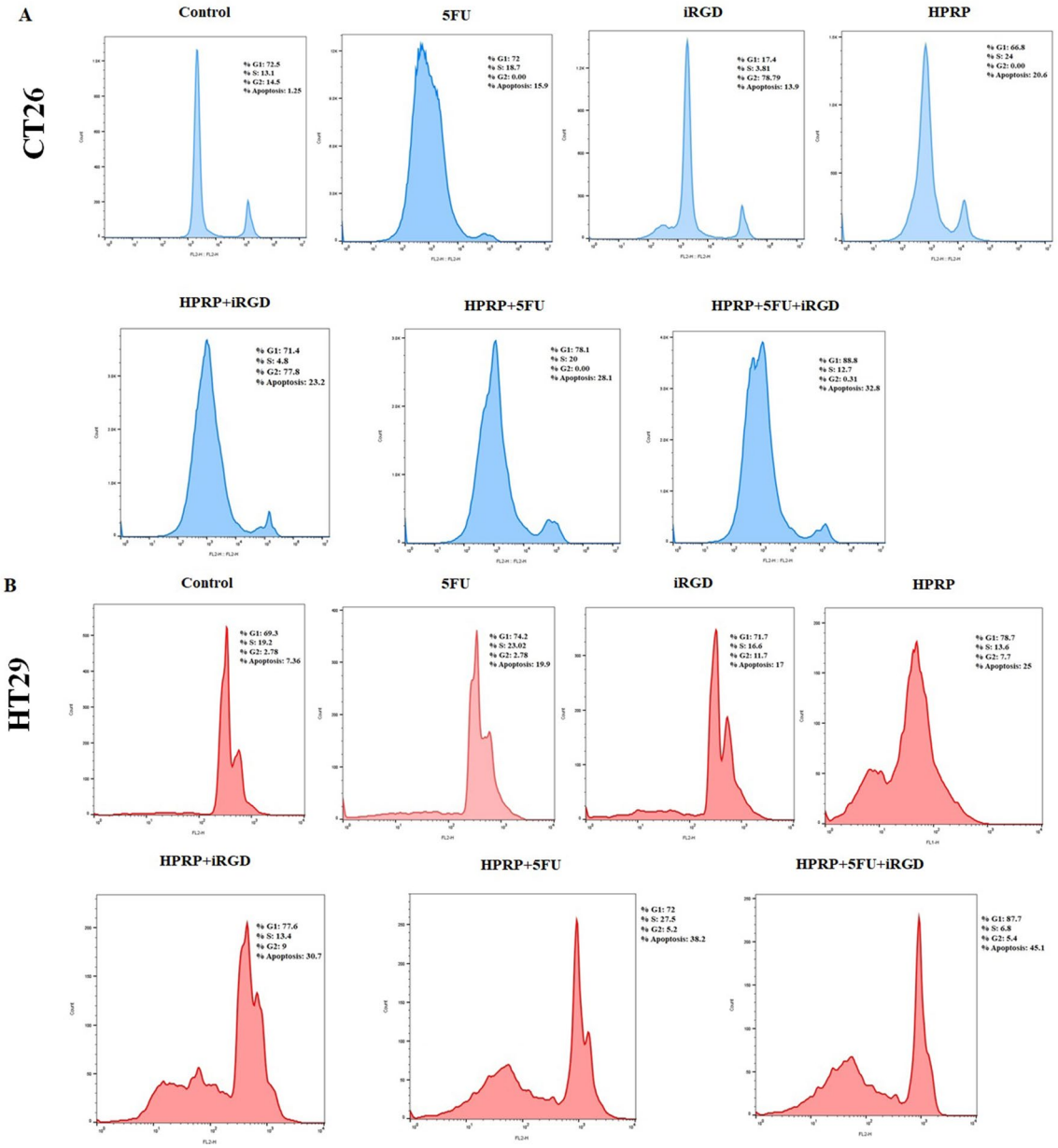

Fig. 3 HPRP-A1 effect on cell cycle of colon cancer cell lines. **(A)** CT26 cells and; **B** HT29 cells were treated with 0.73 µg/ml HPRP-A1 with or without 6 µg/ml iRGD and 3.84×10^{-5} M 5FU for 24 h.Cell cycle analysis using the PI flow cytometry was performed to assess. The percentage of cells in the G1, S, G2-M, and sub-G1 (apoptosis) phases are indicated

However, the expression level of MCP-1 was significantly decreased in the homograft that was treated with HPRP-A1 along with iRGD in comparison to the group that received HPRP-A1or 5FU alone ($P<0.001$) (Fig. 8F). These results indicated that HPRP-A1 had a tumor-suppressive effect on the colon cancer models through disruption of the oxidant/antioxidant balance and upregulation of the pro-inflammatory cytokine that led to the cancer cell death.

Discussion

HPRP-A1 is a 15-mer α-helical cationic peptide with an anticancer activity derived from the N-terminus of ribosomal protein L1 of *H. pylori* (Pütsep et al. 1999). In the present study, for the first time, we investigated the anticancer effect of HPRP-A1 with or without tumor-targeting peptide iRGD and 5 Fluorouracil (5FU) on colon cancer cell lines (CT26 and HT29) and the isograft models of colon cancer. Evidence suggests that HPRP-A1 is able to induce apoptosis through activation of caspase-3, -8, and -9-dependent

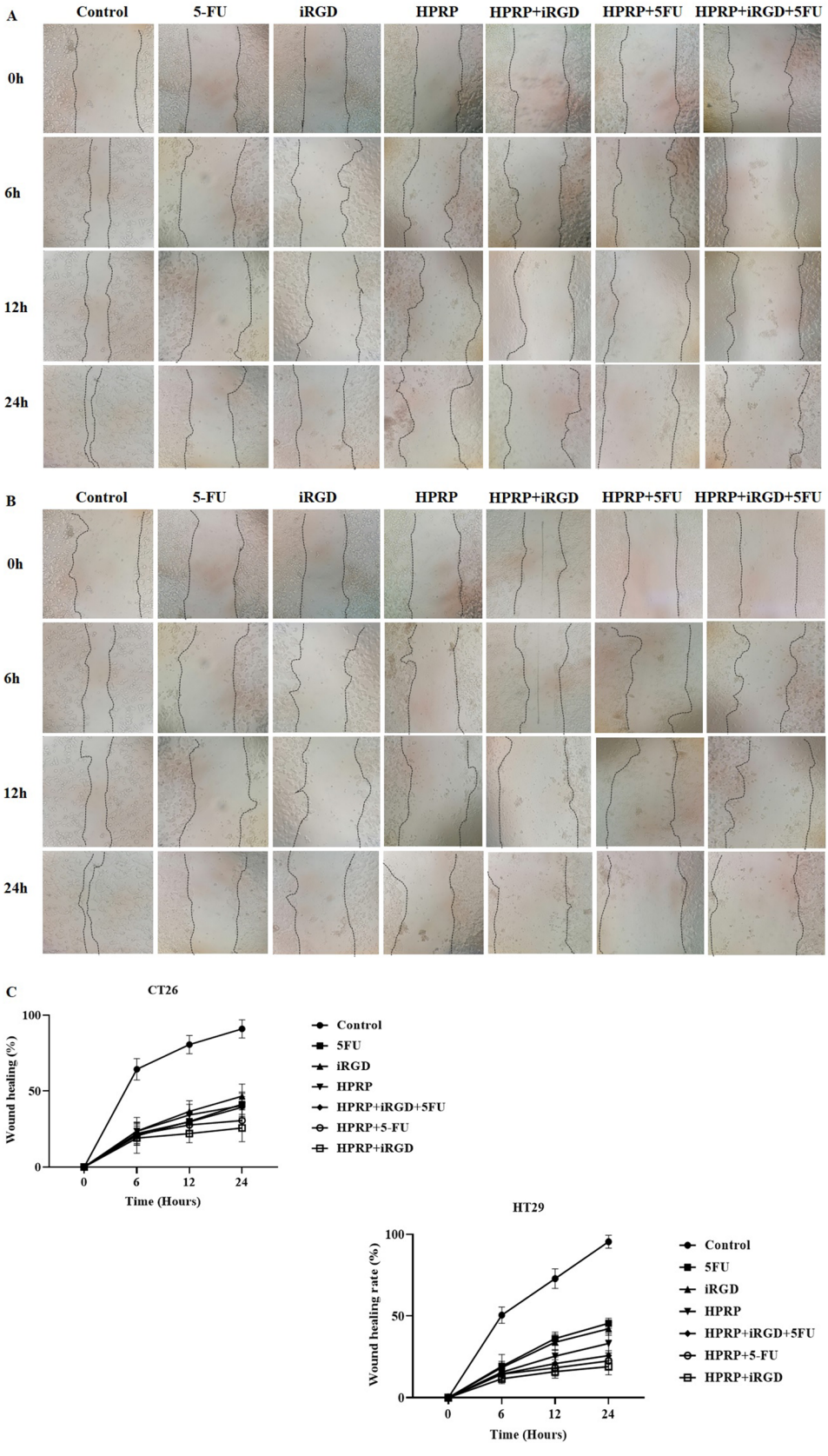

Fig. 4 HPRP-A1inhibits the migration and invasion of colon cancer cells. Inhibition effect of HPRP-A1 on **(A)** CT26 and **B** HT29 after 24 h monitoring (×10 objective; ZEISS Microscopy, Germany). **C** The percentage of wound healing in CT26 and HT29 cells

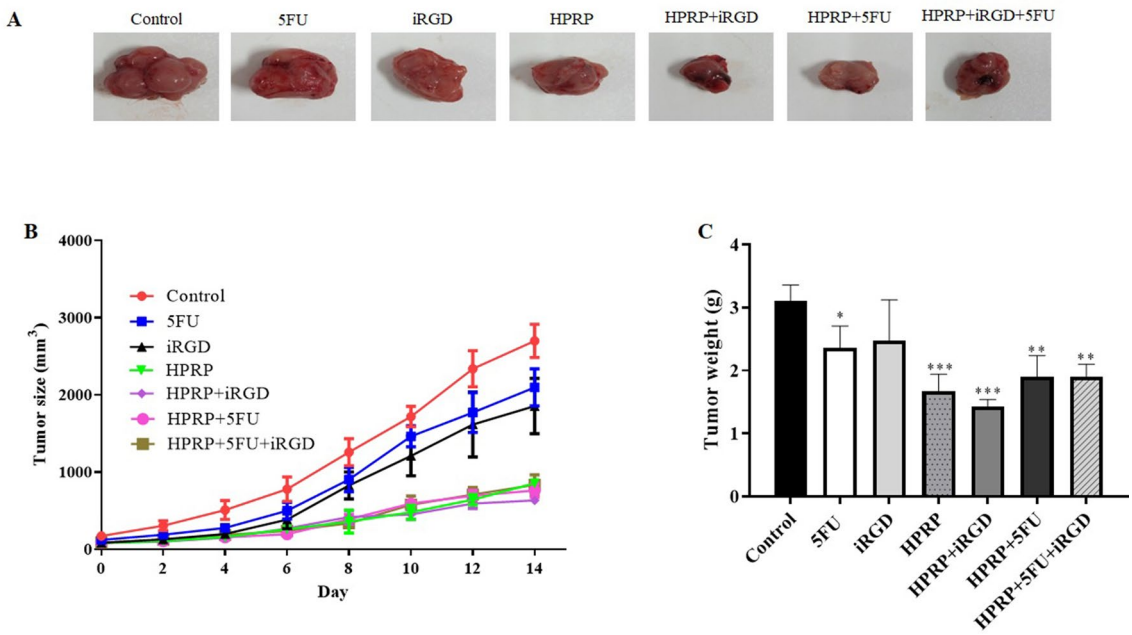

Fig. 5 Effect of HPRP-A1 with or without iRGD and 5FU on inhibiting CT26 cell growth in isograft mice. **A** Representative images of tumors in all treatment groups. **B** Tumor growth measured during the experimental period in each group. **C** Tumor weight of each treatment group. (*$P<0.05$; **$P<0.01$; and ***$P<0.001$ compare to control group)

pathways (Hao et al. 2015). Furthermore, iRGD is well known as an apoptosis-inducing peptide with high penetration into the tumor tissue. HPRP-A1 consider is well known as a membrane-active peptide, that can induce rapid membrane disruption (Hao et al. 2015). The previous study on A549 non-small cell lung cancer cells demonstrated that combination therapy of HPRP-A1 with iRGD caused the destruction of the integrity of the cell membrane and adherence to the mitochondrial net which led to inducing apoptosis in the cancer cells via a caspase-dependent pathway. Furthermore, it demonstrates that cells treated with HPRP-A1 co-administered with iRGD could increase the level of reactive oxygen species (ROS) generation which consider as one of the primary indicators of disruption of the mitochondrial membrane (Hu et al. 2018d). Moreover, the 3D MCS model result in this study indicates that iRGD increase the penetration ability of HPRP-A1 which also enhances the selectivity of the peptide (Hu et al. 2018d). Another study on non-small cell lung cancer (NSCLC) A549 cell line also demonstrates that co-administration of HPRP-A1 with kla-TAT induced much more ROS generation which shows the strong synergistic effect of these two peptides. In addition, the combination therapy leads to more LDH was released from the cytoplasm that indicates the cell membrane was disrupted more seriously (Hu et al. 2018c). However, our results demonstrate that co-administration significantly increased the apoptotic activities of the two peptides, indicating an increase in the rate of early apoptosis in CT26 cells, while combination therapy of these two peptides with 5FU leads to an early higher rate of apoptosis in the HT29 cells. BAX belongs to the BCL2 protein family that contributes to programmed cell death or apoptosis (Kuwana et al. 2005); It is an apoptosis regulator, while BCL2 (B-cell lymphoma 2) has an antiapoptotic activity as the other member of this family that also has a significant role in the resistance of tumor cells to chemotherapy or radiation therapy (Kuwana et al. 2005). Furthermore, BCL2 increased the expansion of neoplastic cells by blocking the turnover of the normal cell via physiological cell death mechanisms. The overexpression of BCL2 as an antiapoptotic gene leads to loss of the tumor suppressor activity of proapoptotic genes such as *Bax, Bak, Bok*. Therefore, restoring the apoptotic process of tumor cells is possible by blocking the expression of BCL2 (Wang et al. 2000). Our results demonstrate that combination therapy of HPRP-A1 with iRGD and 5FU significantly increased the expression of BAX while reducing the expression level of BCL2 in the tumor tissue that leads to an increase in the ratio of apoptosis.

Previous studies demonstrate that HPRP-A1 co-administered with iRGD can induce a G1 arrest on the A549 lung cancer cells (Hu et al. 2018d). Another study also demonstrates that HPRP-A1 in combination with kla-TAT can arrest the A549 cell cycle in the G1 phase and resulted in an increase of cell number in sub-G1 phase. In the present study, the G1 stage arrest was validated with the regulation of cyclin-D1 (Hu et al. 2018c). In addition,

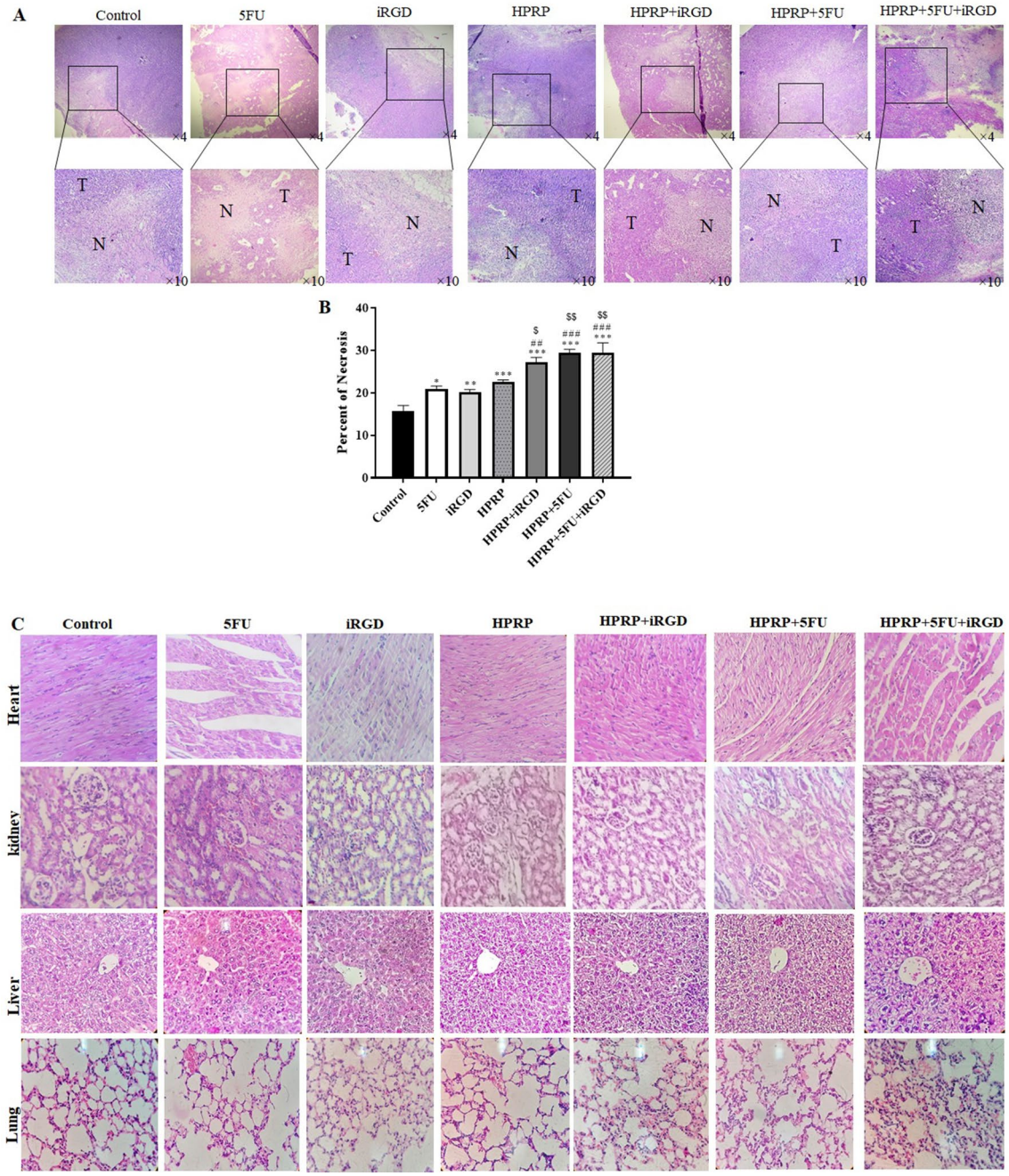

Fig. 6 H&E staining demonstrated microscopic finding showed the tumor necrosis and effect on primary organs from the isograft mice model. **A** The necrosis area is indicated by N and the tumor area show by T in each group. Magnification was mention under each figure. **B** Necrosis percentage of each group. **C** Morphological details of indicated organs were investigated using hematoxylin–eosin staining. No significant pathological changes in heart, liver, kidney, and lung were observed in nude mice following treatment with HPRP-A1 with or without iRGD or/and 5FU. (*$P<0.05$; **$P<0.01$; and ***$P<0.001$ compare to control group); (# ##$P<0.01$ and ###$P<0.001$ compare to 5FU group); and ($P<0.05$ and $$P<0.01$ compare to HPRP-A1 group)

this combination therapy resulted in much higher numbers of cells in sub-G1 of A549 lung cancer cells. Same as the result of previous studies, our results also indicated that coadministration of HPRP-A1 with iRGD and 5FU arrest the CT26 and HT29 cell cycles at G0/G1. Furthermore, this combination therapy increased the number of cells in sub-G1 of both cell lines that caused higher apoptotic activity. In addition, we observed a higher expression level of the p53 in the tumor tissues of the group that received HPRP-A1 and 5FU with or without iRGD, which mediate

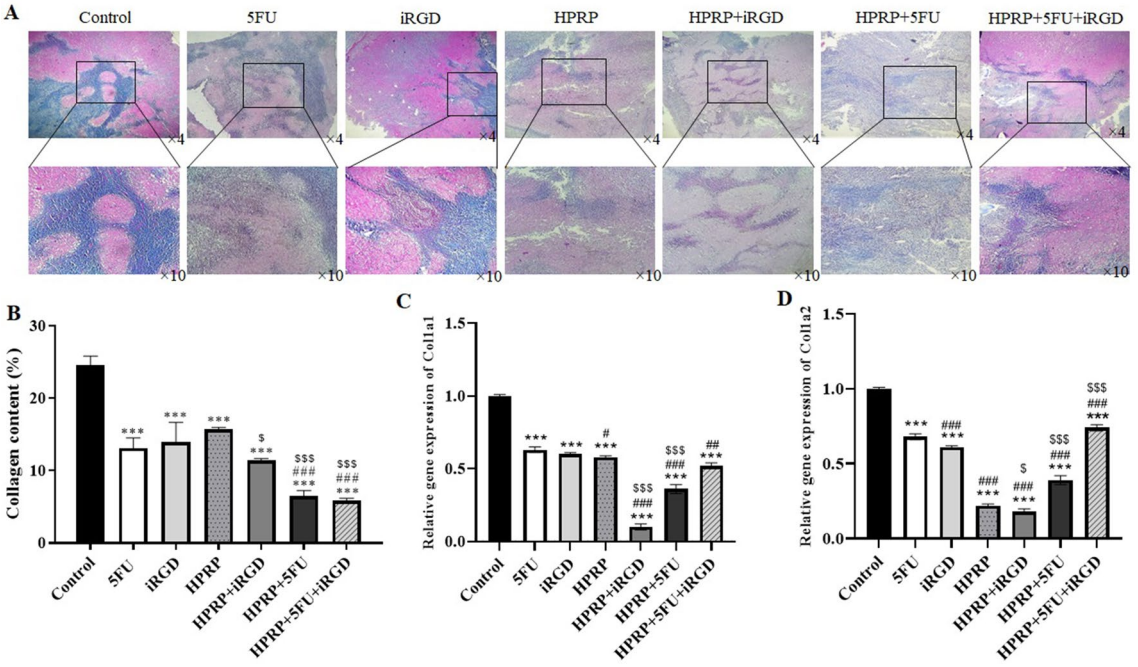

Fig. 7 Trichrome staining indicates the fibrotic area and collagen accumulation in tumor tissue. **A** The blue area shows the fibrotic. **B** The percentage of collagen content of each group. **C** and **D** The expression level of CoL1a1 and CoL1a2 genes in tumor tissue. (***$P<0.001$ compare to control group); (#$P<0.05$; ##$P<0.01$; and ###$P<0.001$ compare to 5FU group); and ($P<0.05$ and $$$P<0.001$ compare to HPRP-A1 group)

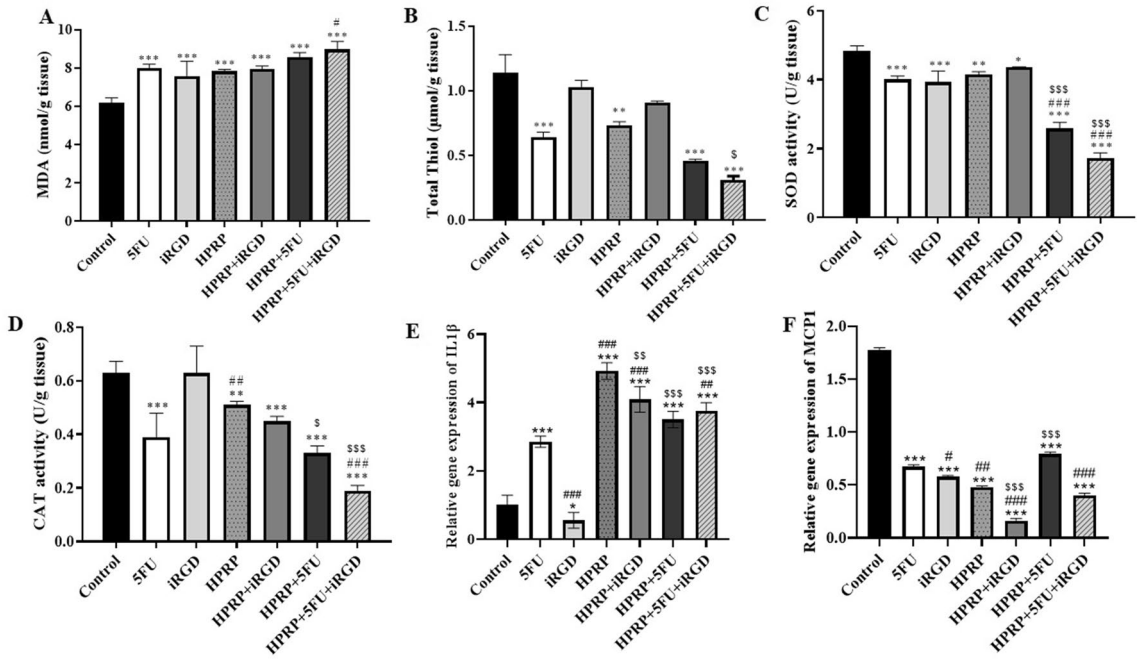

Fig. 8 HPRP-A1 effect on oxidative markers, pro-inflammatory cytokines, and pro-fibrotic gene. The outcomes of HPRP-A1 with or without iRGD or/and 5FU **(A)** MDA, **B** total thiol of the serum, **C** SOD activity, and **D** catalase activity. **E** and **F** HPRP-A1effects on the expression level of pro-inflammatory gene IL1β and the pro-fibrotic gene MCP-1, respectively. (*$P<0.05$; **$P<0.01$; and ***$P<0.001$ compare to control group); (#$P<0.05$; ##$P<0.01$; and ###$P<0.001$ compare to 5FU group); and ($P<0.05$; $$$P<0.01$; and $$$$P<0.001$ compare to HPRP-A1 group) (MDA = Malonyl dialdehyde, SOD = Superoxide dismutase)

the blocking cell cycle progression. The tumor protein "p53" that is also known as TP53, has a role in regulation or progression, apoptosis, and hence functions as a tumor suppression. p53 becomes activated in response to different factors in including DNA damage, oxidative stress, ribonucleotide depletion, and deregulated oncogene expression, etc. (Han et al. 2008). The result of the present study on BALB/c nude mice was subcutaneously injected with A549 cells to create tumors demonstrates that co-administration of HPRP-A1 and iRGD can significantly inhibit tumor proliferation and decrease the tumor size. Furthermore, it demonstrates that HPRP-A1 alone or in co-administration with iRGD did not reflect the body-weight of the A549 xenograft mice (Hu et al. 2018d). The H&E result of this study shows that HPRP-A1 alone or in combination with iRGD has no toxicity against major organs of the A549 xenograft nude mice (Hu et al. 2018d). In line with the previous results, the *in-vivo* results of our study also demonstrate that co-administration of HPRP-A1 with iRGD significantly reduced the tumor size and weight. According to the histological results, the combination therapy of these two peptides with 5FU caused the wider necrotic area in the tumor tissue, while there were no obvious changes in these organs after treatment with HPRP-A1 alone or in combination with iRGD and 5FU. Furthermore, the histological results indicated that combination therapy of HPRP-A1 with iRGD and 5FU significantly decreased the fibrotic area and collagen accumulation in the tumor tissue in comparison to the control group and when the experimental group received single therapy. Therefore, these two peptides can enhance the anti-fibrotic and necrosis activity of 5FU in comparison to the time that the experimental group was treated with 5FU alone. Moreover, a higher expression level of COL1a1and COL1a2 was observed in the group that received peptides along with 5FU. Evidence suggests the overexpression of these two genes in different cancers such as colorectal cancer and medulloblastoma, having a role in tumor invasion and progression. Collagen type I α 1 (COL1A1) and collagen type I α 2 (COL1A2) are known as two chains of type I collagen that are the main members of the collagen family and the main structural components of the extracellular matrix. Changes in the expression levels of COL1A1 and COL1A2 used to predict prognosis in various types of cancer (Shin et al. 2011, 2014). Thus, HPRP-A1 can prevent the invasion and progression in the tumor cells by downregulation of the expression of COL1a1and COL1a2.

The monocyte chemoattractant protein-1 (MCP-1/CCL2) is a member of the C-C chemokine family. MCP-1 is well-known as a pro-inflammatory and pro-fibrotic chemokine, which contributes to tumor initiation and metastasis. Our results show that HPRP-A1 with iRGD has tumor suppressor activity by downregulating the expression of the pro-fibrotic gene MCP-1. IL1β plays a relevant role in anti-tumorigenic effects through inducing both Th1 and Th17 (Haabeth et al. 2011, 2016). We observed the higher expression level of a pro-inflammatory gene such as IL1β in the experimental group receiving HPRP-A1by iRGD with or without 5FU. Our results indicated that peptides have tumor suppressor activity by downregulating the pro-fibrotic gene, upregulating the pro-inflammatory, and disrupting the oxidant/antioxidant balance, including the increasing MDA as an oxidative marker and decreasing the anti-oxidant markers, including thiol, catalase, and SOD. According to these results, HPRP-A1 can be considered as a novel potential agent in the treatment of colon cancer, which also promotes the influence of chemotherapy agents such as 5FU. However, confirming these results requires further studies to indicate the exact anticancer mechanism of HPRP-A1.

Acknowledgements This study was a part of a Ph.D. dissertation by Atieh Yaghoubi.

Funding This research was funded by Mashhad University of Medical Sciences, Mashhad, Iran (981262).

Declarations

Conflict of interest The authors have declared that have no conflict of interest.

References

Abedizadeh R, Rezvan H, Nourian A (2020) A new in vivo model for analysis of colon carcinoma micrometastasis in BALB/c mice. J Shahrekord Univ Med Sci 22(2):88–95

Aebi H (1984) Catalase in vitro. Methods Enzymol 105:121–126

Amerizadeh F, Rezaei N, Rahmani F, Hassanian SM, Moradi-Marjaneh R, Fiuji H et al (2018) Crocin synergistically enhances the anti-proliferative activity of 5-flurouracil through Wnt/PI3K pathway in a mouse model of colitis-associated colorectal cancer. J Cell Biochem 119(12):10250

Boohaker RJ, Lee M, Vishnubhotla P, Perez JLM, Khaled AR (2012) The use of therapeutic peptides to target and to kill cancer cells. Curr Med Chem 19(22):3794–3804

Cao C, Yan TD, Black D, Morris DL (2009) A systematic review and meta-analysis of cytoreductive surgery with perioperative intraperitoneal chemotherapy for peritoneal carcinomatosis of colorectal origin. Ann Surg Oncol 16(8):2152–2165

Chang J, Liu Y, Han B, Zhou C, Bai C, Li J (2015) Pseudomonas aeruginosa preparation plus chemotherapy for advanced non-small-cell lung cancer: a randomized, multicenter, double-blind phase III study. Med Oncol 32(5):139

Cohen E, Ophir I, Shaul YB (1999) Induced differentiation in HT29, a human colon adenocarcinoma cell line. J Cell Sci 112(16):2657–2666

Dinarvand P, Hassanian SM, Weiler H, Rezaie AR (2015) Intraperitoneal administration of activated protein C prevents postsurgical adhesion band formation. Blood 125(8):1339–1348

Elmi S, Sallam NA, Rahman MM, Teng X, Hunter AL, Moien-Afshari F et al (2008) Sulfaphenazole treatment restores

endothelium-dependent vasodilation in diabetic mice. Vascul Pharmacol 48(1):1–8
Fujimori M (2006) Genetically engineered bifidobacterium as a drug delivery system for systemic therapy of metastatic breast cancer patients. Breast Cancer 13(1):27–31
Giovannetti E, Wang Q, Avan A, Funel N, Lagerweij T, Lee JH et al (2014) Role of CYB5A in pancreatic cancer prognosis and autophagy modulation. J Natl Cancer Inst 106(1):djt346
Gontero P, Bohle A, Malmstrom P-U, O'Donnell MA, Oderda M, Sylvester R et al (2010) The role of bacillus Calmette-Guérin in the treatment of non–muscle-invasive bladder cancer. Eur Urol 57(3):410–429
Gupta PK, Tripathi D, Kulkarni S, Rajan M (2016) Mycobacterium tuberculosis H37Rv infected THP-1 cells induce epithelial mesenchymal transition (EMT) in lung adenocarcinoma epithelial cell line (A549). Cell Immunol 300:33–40
Haabeth OAW, Lorvik KB, Hammarström C, Donaldson IM, Haraldsen G, Bogen B et al (2011) Inflammation driven by tumour-specific Th1 cells protects against B-cell cancer. Nat Commun 2(1):1–12
Haabeth OAW, Lorvik KB, Yagita H, Bogen B, Corthay A (2016) Interleukin-1 is required for cancer eradication mediated by tumor-specific Th1 cells. Oncoimmunology 5(1):e1039763
Hamilton AM, Aidoudi-Ahmed S, Sharma S, Kotamraju VR, Foster PJ, Sugahara KN et al (2015) Nanoparticles coated with the tumor-penetrating peptide iRGD reduce experimental breast cancer metastasis in the brain. J Mol Med 93(9):991–1001
Han E-S, Muller FL, Pérez VI, Qi W, Liang H, Xi L et al (2008) The in vivo gene expression signature of oxidative stress. Physiol Genomics 34(1):112–126
Hao X, Yan Q, Zhao J, Wang W, Huang Y, Chen Y (2015) TAT modification of alpha-helical anticancer peptides to improve specificity and efficacy. PLoS ONE 10(9):e0138911
Hao W, Hu C, Huang Y, Chen Y (2019) Coadministration of kla peptide with HPRP-A1 to enhance anticancer activity. PLoS ONE 14(11):e0223738
Hetz C, Bono MR, Barros LF, Lagos R (2002) Microcin E492, a channel-forming bacteriocin from Klebsiella pneumoniae, induces apoptosis in some human cell lines. Proc Natl Acad Sci 99(5):2696–2701
Hu C, Chen X, Huang Y, Chen Y (2018a) Co-administration of iRGD with peptide HPRP-A1 to improve anticancer activity and membrane penetrability. Sci Rep 8(1):2274
Hu C, Huang Y, Chen Y (2018b) Targeted modification of the cationic anticancer peptide HPRP-A1 with iRGD to improve specificity, penetration, and tumor-tissue accumulation. Mol Pharm 16(2):561–572
Hu C, Chen X, Huang Y, Chen Y (2018c) Synergistic effect of the pro-apoptosis peptide kla-TAT and the cationic anticancer peptide HPRP-A1. Apoptosis 23(2):132–142
Hu C, Chen X, Huang Y, Chen Y (2018d) Co-administration of iRGD with peptide HPRP-A1 to improve anticancer activity and membrane penetrability. Sci Rep 8(1):1–14
Kang H-L, Lee W-K, Song J-Y, Choi S-H, Park S-G, Ryu B-D et al (2005) Helicobacter pylori Strain 51 (Korean Isolate): ordered overlapping BAC Library, combined physical and genetic map, and comparative analysis with H. pylori strain 26695 and strain J99. J Microbiol Biotechnol 15(4):844–854
Kuwana T, Bouchier-Hayes L, Chipuk JE, Bonzon C, Sullivan BA, Green DR et al (2005) BH3 domains of BH3-only proteins differentially regulate Bax-mediated mitochondrial membrane permeabilization both directly and indirectly. Mol Cell 17(4):525–535
Lax AJ (2005) Bacterial toxins and cancer—a case to answer? Nat Rev Microbiol 3(4):343
Lecuit M, Abachin E, Martin A, Poyart C, Pochart P, Suarez F et al (2004) Immunoproliferative small intestinal disease associated with Campylobacter jejuni. N Engl J Med 350(3):239–248
Lemoine L, Sugarbaker P, Van der Speeten K (2016) Pathophysiology of colorectal peritoneal carcinomatosis: role of the peritoneum. World J Gastroenterol 22(34):7692
Marjaneh RM, Rahmani F, Hassanian SM, Rezaei N, Hashemzehi M, Bahrami A et al (2018) Phytosomal curcumin inhibits tumor growth in colitis-associated colorectal cancer. J Cell Physiol 233(10):6785–6798
Marqus S, Pirogova E, Piva TJ (2017) Evaluation of the use of therapeutic peptides for cancer treatment. J Biomed Sci 24(1):21
Nath G, Gulati AK, Shukla VK (2010) Role of bacteria in carcinogenesis, with special reference to carcinoma of the gallbladder. World J Gastroenterol: WJG 16(43):5395
Nautiyal J, Kanwar SS, Yu Y, Majumdar AP (2011) Combination of dasatinib and curcumin eliminates chemo-resistant colon cancer cells. J Mol Signal 6(1):1–11
Pütsep K, Brändén C-I, Boman HG, Normark S (1999) Antibacterial peptide from H. pylori. Nature 398(6729):671
Qifan W, Fen N, Ying X, Xinwei F, Jun D, Ge Z (2016) iRGD-targeted delivery of a pro-apoptotic peptide activated by cathepsin B inhibits tumor growth and metastasis in mice. Tumor Biol 37(8):10643–10652
Roberts NJ, Zhang L, Janku F, Collins A, Bai R-Y, Staedtke V et al (2014) Intratumoral injection of clostridium novyi-NT spores induces antitumor responses. Sci Transl Med 6(249):249ra111-249ra111
Ruoslahti E (2017) Tumor penetrating peptides for improved drug delivery. Adv Drug Deliv Rev 110:3–12
Shin K, Lee J, Guo N, Kim J, Lim A, Qu L et al (2011) Hedgehog/Wnt feedback supports regenerative proliferation of epithelial stem cells in bladder. Nature 472(7341):110–114
Shin K, Lim A, Zhao C, Sahoo D, Pan Y, Spiekerkoetter E et al (2014) Hedgehog signaling restrains bladder cancer progression by eliciting stromal production of urothelial differentiation factors. Cancer Cell 26(4):521–533
Siegel RL, Miller KD, Jemal A (2020) Cancer statistics, 2020. CA: Cancer J Clin 70(1):7–30
Sugahara KN, Teesalu T, Karmali PP, Kotamraju VR, Agemy L, Girard OM et al (2009) Tissue-penetrating delivery of compounds and nanoparticles into tumors. Cancer Cell 16(6):510–520
Sugahara KNTT, Karmali PP, Kotamraju VR, Agemy L, Greenwald DR, Ruoslahti E (2010) Coadministration of a tumor-penetrating peptide enhances the efficacy of cancer drugs. Science 328(5981):1031–1035
Sugarbaker PH (2016) Improving oncologic outcomes for colorectal cancer at high risk for local–regional recurrence with novel surgical techniques. Expert Rev Gastroenterol Hepatol 10(2):205–213
Teesalu TSK, Kotamraju VR, Ruoslahti E (2009) C-end rule peptides mediate neuropilin-1-dependent cell, vascular, and tissue penetration. PNAS 106(38):16157–16162
Teesalu T, Sugahara KN, Ruoslahti E (2013) Tumor-penetrating peptides. Front Oncol 3:216
Wang J-L, Liu D, Zhang Z-J, Shan S, Han X, Srinivasula SM et al (2000) Structure-based discovery of an organic compound that binds Bcl-2 protein and induces apoptosis of tumor cells. Proc Natl Acad Sci 97(13):7124–7129
Wei MQ, Ellem KA, Dunn P, West MJ, Bai CX, Vogelstein B (2007) Facultative or obligate anaerobic bacteria have the potential for multimodality therapy of solid tumours. Eur J Cancer 43(3):490–496
Yan L, Kanada M, Zhang J, Okazaki S, Terakawa S (2015) Photodynamic treatment of tumor with bacteria expressing killerred. PLoS ONE 10(7):e0131518
Zhang Y, Davis C, Ryan J, Janney C, Peña MMO (2013) Development and characterization of a reliable mouse model of colorectal cancer metastasis to the liver. Clin Exp Metas 30(7):903–918

Zhao M, Yang M, Ma H, Li X, Tan X, Li S et al (2006) Targeted therapy with a Salmonella typhimurium leucine-arginine auxotroph cures orthotopic human breast tumors in nude mice. Can Res 66(15):7647–7652